Optical and Quantum Electronics (2021) 53:72
https://doi.org/10.1007/s11082-020-02709-7

TCAD based performance assessment of Indium Gallium Nitride based single junction solar cells for different mole fractions of Indium

Varun Chandra[1,2] · Arun Dev Dhar Dwivedi[1] · Nidhi Sinha[1]

Received: 19 August 2020 / Accepted: 21 December 2020 / Published online: 22 January 2021
© The Author(s), under exclusive licence to Springer Science+Business Media, LLC part of Springer Nature 2021

Abstract
The tailoring the band gap energy of the ternary Indium Gallium Nitride ($In_xGa_{(1-x)}N$) alloy shows a good spectral match with a range of wavelength in electromagnetic spectrum and provided a new approach for its utilization in Photovoltaic solar cells. In this paper a 2D numerical simulation of Indium Gallium Nitride ($In_xGa_{1-x}N$) single junction solar cell using TCAD has been presented. The device has been simulated and analyzed using physical models such as Auger recombination models using Fermi–Dirac Statistics, Shockley–Read–Hall recombination models and Band Gap Narrowing effect. The J–V and P–V characteristics of the device in dark and illuminated condition were analyzed. The single-junction $In_{0.72}Ga_{0.28}N$ solar cell shows the maximum efficiency under normalized AM 1.5 G, 0.1 W/cm^2 and at a temperature of 300 K. Further, figure of merits depending on different mole fraction of Indium, like short current density (J_{sc}), Open circuit Voltage (V_{oc}), fill factor (FF), maximum power generated (P_{max}) and conversion efficiency of the designed solar cell has been extracted.

Keywords TCAD · InGaN · Solar cell · ARC · Numerical simulation · Silvaco

1 Introduction

Indium Gallium Nitride ($In_xGa_{1-x}N$) a direct band gap compound semiconductor material covers a wide range of solar spectrum from ultraviolet to near infrared wavelengths (Kazazis et al. 2018). They can achieve a band gap spanning from 0.7 to 3.4 eV. This unique property of InGaN provides a good opportunity to design novel devices. Gallium (Ga) riched InGaN alloys already been the heart of LED's, laser diodes where as Indium rich InGaN alloys could be utilized for high efficiency multi-junction solar cells due to high tolerance to radiation (Polyakov et al. 2013), high mobility (Mesrane et al. 2015) and large absorption coefficient (Matioli et al. 2011; Lin et al. 2012). The technology of

✉ Arun Dev Dhar Dwivedi
adddwivedi@gmail.com

[1] School of Electronics Engineering (SENSE), VIT University, Vellore, TN 632014, India

[2] Department of Electrical and Electronics Engineering, Poornima University, Jaipur, India

III-V nitrides had shown its ability that can be utilized for manufacturing high efficiency photovoltaics depending on the mole fraction(x) of Indium.

$In_xGa_{1-x}N$ covers the entire AM 1.5 spectrum indicating its exceptionally tenacious and robust photoluminescence irrespective of growing on lattice mismatched substrates. The optical and electronic propertiesof $In_xGa_{1-x}N$ alloys exhibit a much higher resistance tohigh-energy (2 MeV) photon irradiation than currently used PV materials such as GaAs, GaInP, offering great potential for a radiation-hard high-efficiency solar cell for space applications (Bhuiyan et al. 2012). The performance of InGaN was investigated extensively after the revision of InN band gap energy for a solar cell since 2003 (Mesrane et al. 2015; Wu et al. 2003; Jani et al. 2005; Hamzaoui et al. 2005; Anani et al. 2007; Zhang et al. 2007; Islam et al. 2008; Anani et al. 2009; Caselli 2012; Vilbois et al. 2012; Boudaoud et al. 2015; Abdoulwahab et al. 2016). Still there are many challenges to be faced in order to achieve the goal of high efficiency solar cells from all different view point. The drawbacks such as difficulty in p-doping due to high residual donors concentration (Dahal et al. 2009), in realizing ohmic contacts (Bhuiyan et al. 2012), impact on layer quality due to complex technological processes (Meng et al. 2010; Gherasoiu et al. 2014), difficulty in growing InGaN with Indium composition high enough to cover the whole solar spectrum (Yamamoto et al. 2013; Durukan et al. 2015). Due to aforesaid drawbacks the InGaN thin film solar cell is still in early stages of development and the efficiency reported in literature is still low to be competitive with established thin film solar cells. Because of this we present a comparative study of single PN junction structures using realistic physical models and mathematical optimization approaches based on different mole fraction of Indium content varying from 0.58 to 0.9.

This paper is organized as follows: Sect. 2 introduces the theoretical modeling and simulation of InGaN. In Sect. 3, we have shown dependency of figures of merits of solar cells on Indium composition and Sect. 4 includes the conclusion.

2 Theoretical modeling and simulation of InGaN

2.1 Structure

Above Fig. 1 illustrates the Single Junction Indium Gallium Nitride based Solar cell which is modeled using two dimensional numerical simulation tool ATLAS™ from Silvaco which is a physically based two and three dimensional device simulator used to predict the electrical behavior of defined semiconductor structures. This Structure

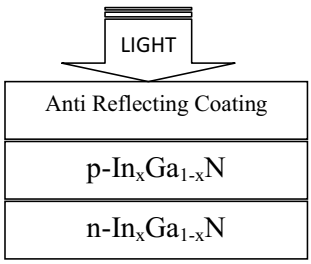

Fig. 1 Structure of single junction Indium Gallium Nitride based solar cell

consists of P-type emitter and N-type base. The anti reflecting coating is considered perfect without any reflection losses. The simulations were performed under 1 Sun at 300 K and AM 1.5 illumination conditions as shown in Fig. 2.

2.2 Physical and optical properties

The Band Gap energy for various mole fractions were calculated based on Indium composition(x) at a temperature 300 K is given by Nawaz and Ahmad (2012):

$$E_g\left(In_xGa_{1-x}N\right) = x \cdot E_g(InN) + (1-x) \cdot E_g(GaN) - b \cdot x \cdot (1-x) \tag{1}$$

where the band gap of InN and GaN are 0.7 eV and 3.42 eV respectively, b is the bowing parameter which is (b = 1.43).

The dependence of the band gap energy on temperature is modeled in Silvaco Atlas is as follows (Silvaco Data systems 2018)

$$E_g\left(T_L\right) = E_{g300}\left(In_xGa_{1-x}N\right) + E_{g\alpha}\left[\frac{300^2}{300 + E_g\beta} - \frac{T_L^2}{T_L + E_g\beta}\right] \tag{2}$$

where E_{g300} is calculated using (1). $E_{g\alpha}$ and $E_{g\beta}$ are material dependent parameters used in single junction solar cell.

The various parameters required for modeling of the $In_xGa_{1-x}N$ based single junction solar cell were calculated from these equations.

Electron Affinity (χ) (Zhang et al. 2007; Li et al. 2009):

$$\chi\left(In_xGa_{1-x}N\right) = 4.1 + 0.7\left(3.4 - E_g\right). \tag{3}$$

Relative Permittivity (ε) (Nawaz et al. 2012):

$$\varepsilon\left(In_xGa_{1-x}N\right) = 15.3x + 8.9(1-x). \tag{4}$$

Electron and Hole effective masses (m_n or m_h) (Silvaco Data systems 2018):

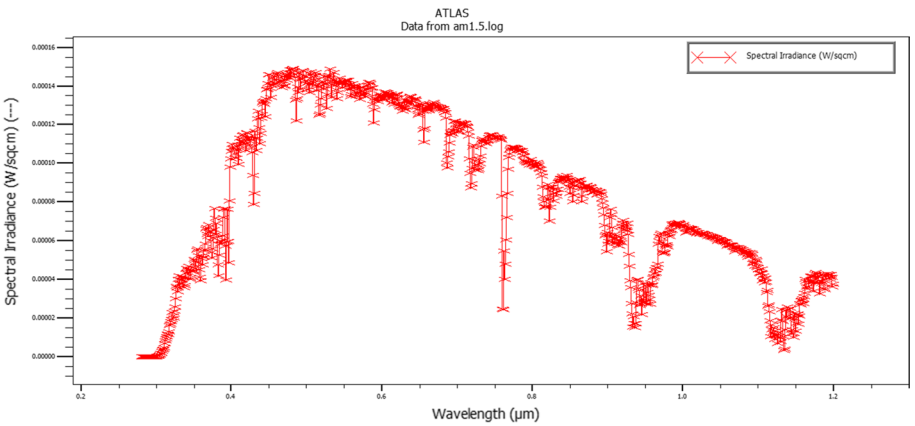

Fig. 2 Graph of global solar spectrum of AM1.5 for Indium Gallium Nitride

$$m_n\left(\mathrm{In}_x Ga_{1-x}\mathrm{N}\right) = 0.12x + 0.2(1-x) \tag{5}$$

$$m_h\left(\mathrm{In}_x Ga_{1-x}\mathrm{N}\right) = 0.17x + 1.0(1-x). \tag{6}$$

Effective density of states in the conduction and valence band (Nc or Nv) (Zhang et al. 2007; Li et al. 2009):

$$N_c\left(\mathrm{In}_x Ga_{1-x}\mathrm{N}\right) = (0.9x + 2.3(1-x)) \times 10^{18} \tag{7}$$

$$N_v\left(\mathrm{In}_x Ga_{1-x}\mathrm{N}\right) = (5.3x + 1.8(1-x)) \times 10^{19}. \tag{8}$$

2.3 Transport modeling

The electron and hole mobility required for drift diffusion model were calculated using Caughey-Thomas expressions (Schwierz 2005):

$$\mu_m = \mu_{1m}\left(\frac{T}{300}\right)^{\alpha_m} + \frac{\mu_{2m}\left(\frac{T}{300}\right)^{\beta_m} - \mu_{1m}\left(\frac{T}{300}\right)^{\alpha_m}}{1 + \left(\frac{N}{N_m^{crit}\left(\frac{T}{300}\right)^{\gamma_m}}\right)^{\delta_m}} \tag{9}$$

where m is n or p, μ_n being the electrons mobility and μ_p holes mobility. T, the absolute temperature, N the doping concentration, α, β, δ, and γ are the model parameters depending on the composition of Indium(x) (Brown et al. 2010).Also, the Auger recombination models using Fermi–Dirac Statistics (Bertazzi et al. 2010), Shockley–Read–Hall recombination models (Ryu et al. 2009) and Band Gap Narrowing effect were included in physical modeling.

2.4 Light absorption modeling

Modeling of Indium Gallium Nitride based solar cell requires a precise model of light absorption for all Indium composition for the whole solar spectrum by using previously proposed model (Brown et al. 2010) as:

$$\alpha\left(\mathrm{In}_x Ga_{1-x}\mathrm{N}\right) = 10^5\sqrt{C\left(E_{ph} - E_g\right) + D\left(E_{ph} - E_g\right)^2}\ \mathrm{cm}^{-1} \tag{10}$$

where E_{ph} is incoming photon energy, E_g material band gap, C and D are empirical parameters depending on the alloy composition given by Farahmand et al. (2001):

$$\mathrm{C} = 3.525 - 18.29x + 40.22x^2 - 37.52x^3 + 12.77x^4 \tag{11}$$

$$\mathrm{D} = -0.6651 + 3.616x - 2.460x^2. \tag{12}$$

Adachi's wavelength dependent refractive index model defined for InGaN for a given photon energy was calculated as Nawaz et al. (2012) and Silvaco Data systems (2018):

$$n(E_{ph}) = \sqrt{A\left(\frac{E_{ph}}{E_g}\right)^{-2}\left\{2 - \sqrt{1+\frac{E_{ph}}{E_g}} - \sqrt{1-\frac{E_{ph}}{E_g}}\right\} + B} \tag{13}$$

where A and B is calculated using Nawaz and Ahmad (2012):

$$\mathrm{A}\left(\mathrm{In}_x\mathrm{Ga}_{1-x}\mathrm{N}\right) = 13.55x + 9.31(1-x) \tag{14}$$

$$\mathrm{B}\left(\mathrm{In}_x\mathrm{Ga}_{1-x}\mathrm{N}\right) = 2.05x + 3.03(1-x). \tag{15}$$

The absorption coefficient and refractive index value required for simulation were obtained for different mole fractions using MATLAB software and is used in Atlas Silvaco. The nitride low filed mobility model parameters were linearly interpolated from the values given in Farahmand et al. (2001). As the experimental values for hole concentration is not available it is assumed same as of GaN. The various parameters considered are shown in Table 1.

2.5 Simulation methodology

The $\mathrm{In}_x\mathrm{Ga}_{1-x}\mathrm{N}$ based single junction solar cell for different mole fractions (x=0.20 to 0.96) are simulated utilizing drift diffusion model in ATLAS™ device simulation software from the Silvaco suite. ATLAS™ solves the drift–diffusion nonlinear partial differential problem considering the Newton coupled and the Gummel decoupled methods (Selberherr 2012; Dwivedi 2010, 2011a, b, 2014; Dwivedi et al. 2010, 2015a, b, 2019, 2020; Sinha et al. 2016a, b; Devarakonda et al. 2020; Dwivedi and Kumari 2020; Dwivedi and Chakrabarti 2007, 2008, 2011, 2015) along with Poisson's and Continuity equations. The Poisson equation is Dwivedi (2010, 2011a, b, 2014), Dwivedi et al. (2010, 2015a, b, 2019, 2020), Sinha et al. (2016a, b), Devarakonda et al. (2020), Dwivedi and Kumari (2020) and Dwivedi and Chakrabarti (2008, 2011, 2015, 2007):

$$\frac{\partial^2\varphi(x)}{\partial x^2} = \frac{q}{\varepsilon}\left[n(x) - p(x) - N_d^+ + N_a^-\right] \tag{16}$$

where φ (x) is potential related to electron n(x) and hole densities p(x). In Silvaco Atlas simulation, the intrinsic Fermi potential is always taken as the reference potential. The electric field is given by

$$\mathrm{E} = -\nabla\psi. \tag{17}$$

The continuity equations used for electrons and holes are given as Dwivedi (2010, 2011a, b, 2014), Dwivedi et al. (2010, 2015a, b, 2019, 2020), Sinha et al. (2016a, b),

Table 1 Parameters used in simulation of $\mathrm{In}_x\mathrm{Ga}_{1-x}\mathrm{N}$

Parameters	Values
Auger recombination for electrons and holes	1.5×10^{-30} cm^6 s^{-1}
Electrons and holes lifetimes	1 ns
Surface recombination velocities	10^3 cm s^{-1}
$\mathrm{N_A}$	6×10^{18} cm^{-3}
$\mathrm{N_D}$	6×10^{18} cm^{-3}

Devarakonda et al. (2020), Dwivedi and Kumari (2020) and Dwivedi and Chakrabarti (2007, 2008, 2011, 2015):

$$\frac{\partial n(x,t)}{\partial t} = G_N - R_N + \frac{1}{q}\frac{\partial}{\partial x}J_N(x) \tag{18}$$

$$\frac{\partial p(x,t)}{\partial t} = G_P - R_P - \frac{1}{q}\frac{\partial}{\partial x}J_P(x) \tag{19}$$

where $J_N(x)$ is electron current density and $J_P(x)$ is hole current density, and G_N and G_P is generation rate of the electrons and holes respectively.

The drift–diffusion model for current densities is given by:

$$J_N = qn\mu_N E_N + qD_N \nabla n \tag{20}$$

$$J_P = qn\mu_P E_P - qD_P \nabla p \tag{21}$$

D_N and D_P represent the diffusion constants, E_N and E_P indicates the local electric fields, ∇n and ∇p represents the 3D spatial gradient of electrons and holes respectively.

Luminous, which is an integral part of the Silvaco ATLAS™ has been used for optical characterization, to determine the photogeneration in the structure. It utilizes ray tracing method, to obtain the optical intensity using refractive index (n) and the extinction coefficient (k).

The simulation uses the source of light and the expression for the source photocurrent is given by (Devarakonda et al. 2020)

$$I_s = q\frac{B_n\lambda}{hc}W_t \tag{22}$$

where B_n is the intensity of the beam number n, λ represents the source wavelength, W_t is the width of the beam.

The available photocurrent in the device is expressed as follows (Devarakonda et al. 2020)

$$I_A = q\frac{B_n\lambda}{hc}\sum_{i=1}^{N_R} W_R \int_0^{Y_i} P_i\alpha_i e^{-\alpha_i y}dy \tag{23}$$

where W_R is the width of the ray, α_i is the absorption coefficient in the material, N_R is the number of rays traced, P_i is the attenuation before the ray starts, Y_i is the length of the ray.

Newton and Gummel method with transfer matrix is used to calculate the electrical and optical characteristics of the device. Luminous, an integral part of ATLAS uses ray tracing method to determine the photogeneration in the structure at each mesh point.

The solar cell analyzed characteristics were the spectral response, the J-V characteristics, P–V characteristics and dependency of efficiency, current density, fill factor and open circuit voltage with different Indium compositions. Table 2 shows the various parameter values used in simulation for different compositions of Indium.

Table 2 Parameters depending on different indium compositions

$In_xGa_{1-x}N$	Permittivity	Affinity	Band gap (eV)
$x=0.20$	3.22	4.6270	2.6472
$x=0.30$	4.73	4.8674	2.3037
$x=0.38$	5.938	5.0454	2.0495
$x=0.42$	6.542	5.1295	1.9293
$x=0.50$	7.75	5.2882	1.7025
$x=0.55$	8.505	5.3809	1.5701
$x=0.58$	8.9580	5.4342	1.4941
$x=0.60$	9.26	5.4686	1.4448
$x=0.68$	10.4680	5.5985	1.2592
$x=0.72$	11.072	5.6587	1.1733
$x=0.78$	11.978	5.7429	1.0530
$x=0.84$	12.884	5.8199	0.9430
$x=0.92$	14.092	5.9114	0.8124
$x=0.96$	14.696	5.9523	0.7539

3 Results and discussions

P-layer and N-layer thickness considered for the study of single junction solar cell based on $In_xGa_{1-x}N$ are 160 nm and 400 nm. The dependency of the $In_xGa_{1-x}N$ single junction solar cell conversion efficiency, fill factor, current density and open circuit voltage on Indium composition were investigated and result were analyzed as shown below. Table 3 Shows the Output characteristics obtained for aforesaid figure of merits of the solar cells under consideration.

Table 3 Figure of merits of $In_xGa_{1-x}N$ for various mole fractions (x) at 300 K

Indium (x)	Figure of merits of $In_xGa_{1-x}N$				
	J_{sc} (mA/cm^2)	V_{oc} (v)	FF (%)	Efficiency (%)	P_{max} (mW/cm^2)
0.2	4.23	0.6418	80.21	2.61	2.18
0.3	9.86	1.7004	84.41	16.94	14.16
0.38	12.53	1.4502	84.48	18.36	15.35
0.42	14.35	1.3352	84.32	19.33	16.16
0.5	21.03	1.1189	83.74	23.58	19.71
0.55	30.59	0.9962	83.01	30.27	25.31
0.58	39.76	0.9273	82.38	36.33	30.38
0.6	43.48	0.8806	81.94	37.53	31.38
0.62	45.45	0.8336	81.58	36.98	30.91
0.68	52.36	0.7009	80.25	35.23	29.46
0.72	66.27	0.6216	79.15	39.004	32.61
0.78	75.85	0.5057	76.99	35.33	29.54
0.84	79.13	0.3985	74.11	27.95	23.37
0.92	91.31	0.2735	68.39	20.43	17.08
0.96	93.74	0.2170	64.21	15.63	13.06

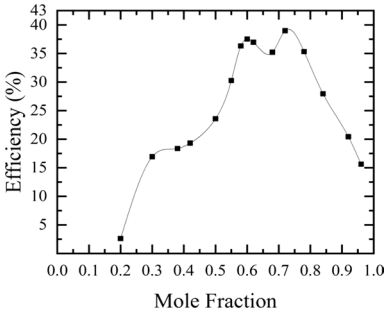

Fig. 3 Graph between efficiency and mole fraction of Indium in InGaN

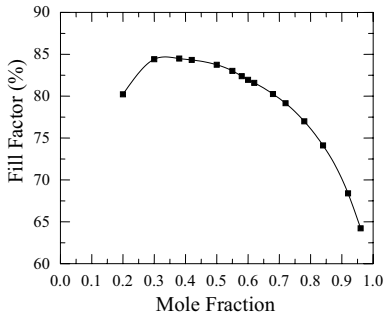

Fig. 4 Graph between Fill Factor and mole fraction of Indium in InGaN

3.1 Effect of Indium composition on conversion efficiency (η)

The Fig. 3 shows the effect of Indium composition on conversion efficiency. It was observed that the conversion efficiency shows the increasing trend till $x=0.72$ and then decreasing trend. The best efficiency is observed at Indium Composition for 0.72.

3.2 Effect of Indium composition on fill factor

The Fig. 4 shows the effect of Indium composition on fill factor.

3.3 Effect of Indium composition on Open Circuit Voltage (V_{oc})

The Fig. 5 shows the effect of Indium composition on open circuit voltage. It was observed that the open circuit voltage shows the increasing trend till $x=0.30$ and then a continuous decreasing trend.

3.4 Effect of Indium composition on current density (J_{sc})

The Fig. 6 shows the effect of Indium composition on current density. It was observed that the current density shows the increasing trend.

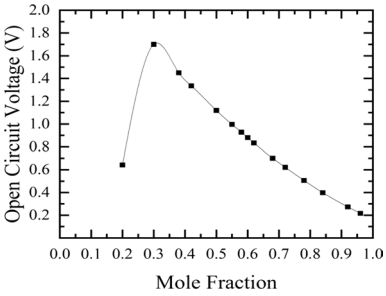

Fig. 5 Graph between open circuit voltage and mole fraction of Indium in InGaN

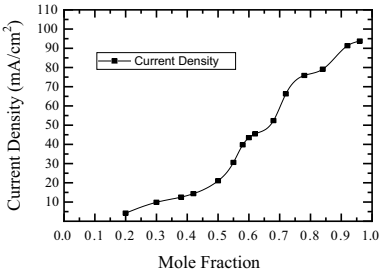

Fig. 6 Graph between current density and mole fraction of Indium in InGaN

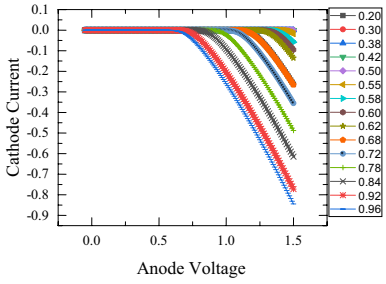

Fig. 7 I–V characteristics in dark condition

3.5 Dark Characteristics of Indium Gallium Nitride

The graph below in Fig. 7 illustrates the dark characteristics of the InGaN single junction solar cell.

3.6 Light characteristics of Indium Gallium Nitride

The graph shown below in Fig. 8 illustrates the I-V characteristics of the InGaN single junction solar cell in illuminated condition for various mole fraction varying from $x = 0.20$ to 0.90.

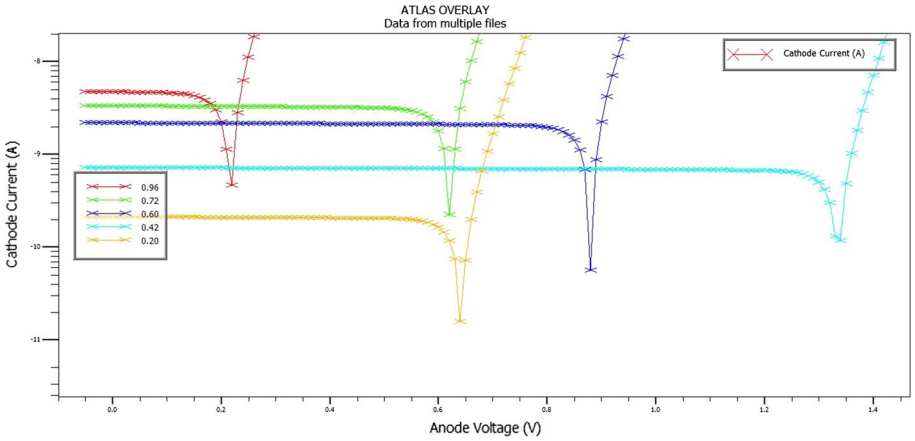

Fig. 8 I–V Characteristics in illuminated condition (current is in log scale)

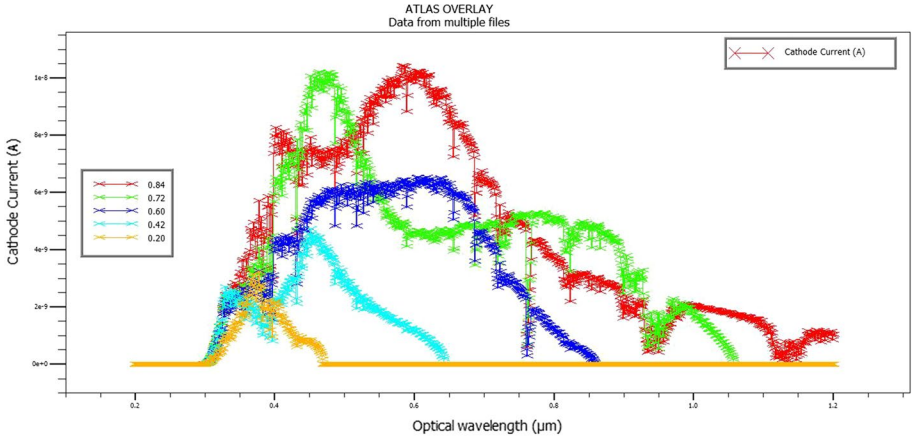

Fig. 9 Spectral response of the InGaN based solar cells

3.7 Spectral response of Indium Gallium Nitride

The graph below in Fig. 9 illustrates the Spectral Response of the InGaN single junction solar cell for Indium composition varying from 0.20 to 0.84.

3.8 Conduction and valence band energy of $In_{0.72}Ga_{0.28}N$

The graph below in Fig. 10 illustrates the energy band diagram of the $In_{0.72}Ga_{0.28}N$ based single junction solar cell.

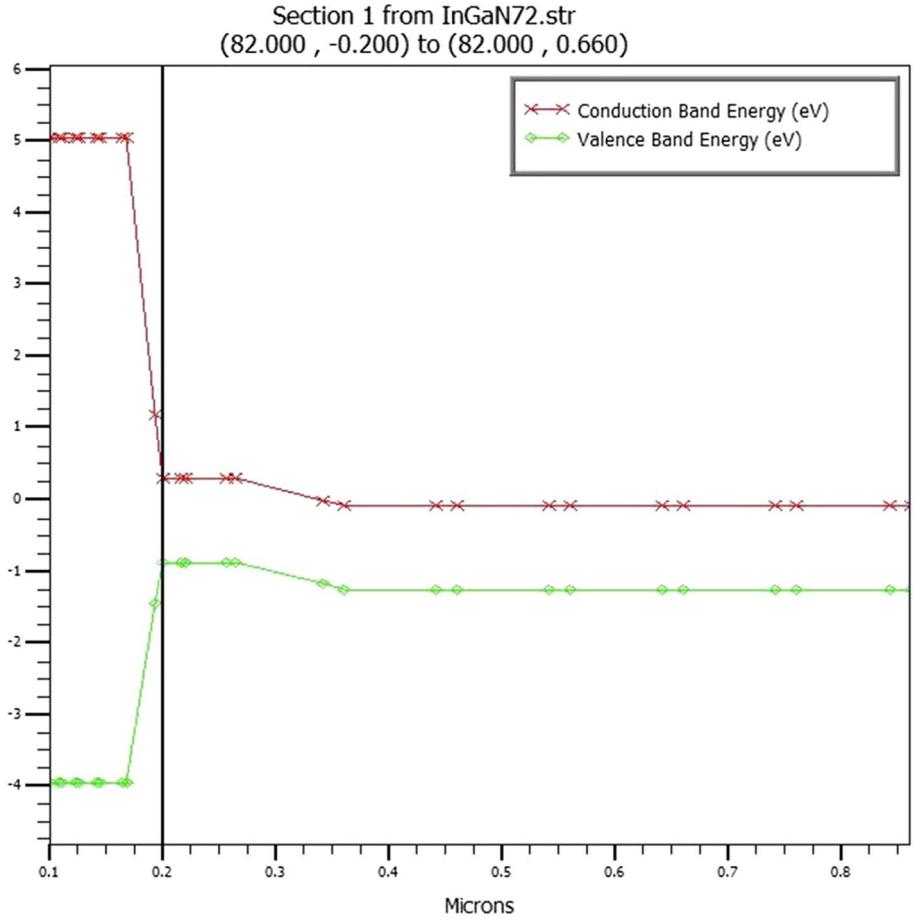

Fig. 10 Energy band diagram of the $In_{0.72}Ga_{0.28}N$ based single junction solar cell

3.9 Photon generation and absorption rate of $In_{0.72}Ga_{0.28}N$

The graph below in Fig. 11 illustrates photon generation and absorption rate at different regions of the device.

3.10 External quantum efficiency of Indium Gallium Nitride

Figure 12 illustrates the external Quantum efficiency curve of InGaN single junction solar cell with wavelength from 0.2 to 1.2 μm for various mole fraction of Indium in InGaN such as 0.20, 0.38, 0.50, 0.60, 0.72, 0.84 and 0.96.

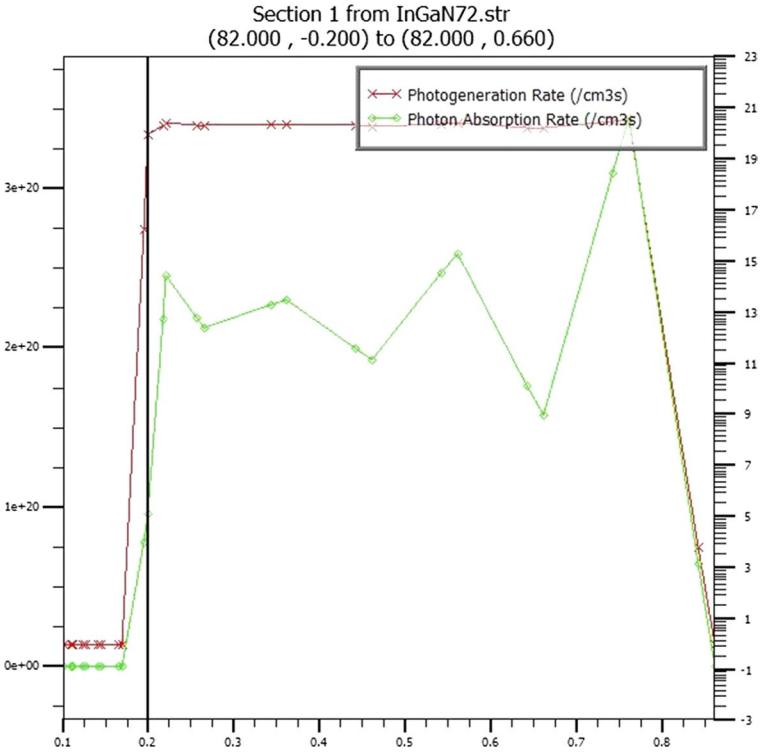

Fig. 11 Photon generation and absorption rate

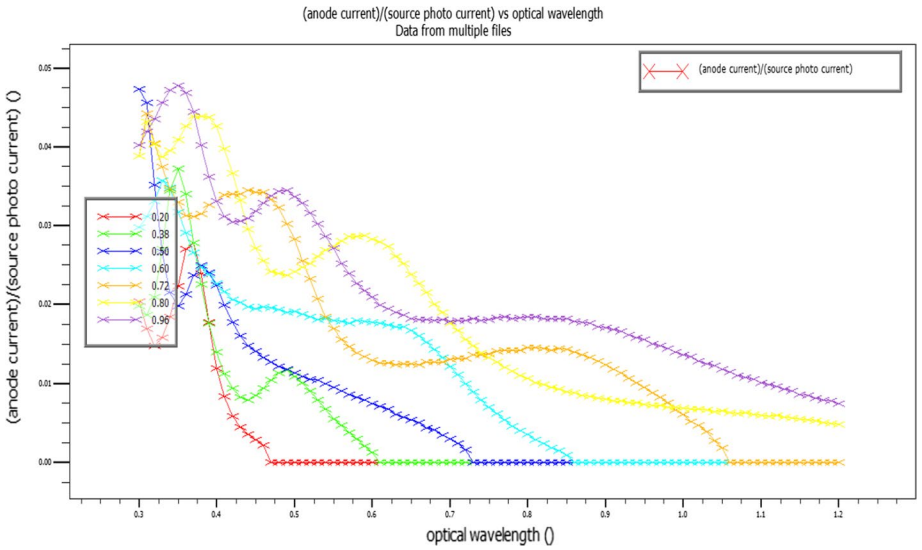

Fig. 12 EQE versus wavelength plot for of Indium Gallium Nitride based solar cell

4 Conclusion

In this paper we have investigated the effect of the mole fraction of Indium on the open circuit voltage, current density, fill factor and conversion efficiency. We observed that the current density shows the increasing nature while fill factor and open circuit voltage has decreasing nature. Considering the best possible efficiency, at mole fraction of 0.72 of Indium the efficiency calculated is 39%. InGaN could be utilized in the Solar cells manufacturing. Future works could be explored on tandem configuration along with different substrate utilization and effect of variation in temperature.

Acknowledgements The authors are thankful to SERB DST Govt. of India for financial support under the Project No. ECR/2017/000179.

References

Abdoulwahab, A., Hamady, S.O.S., Fressengeas, N.: Simulation study of a new InGaN p-layer free schottky based solar cell. Superlattices Microstruct. **96**, 121–133 (2016)

Anani, M., Abid, H., Chama, Z., Mathieu, C., Sayede, A., Khelifa, B.: $In_xGa_{1-x}N$ refractive index calculations. Microelectron. J. **38**(2), pp. 262–266 (2007). ISSN 0026-2692. https://doi.org/10.1016/j.mejo.2006.11.001

Anani, M., Mathieu, C., Khadraoui, M., Zouaoui, C., Lebid, S., Amar, Y.: High-grade efficiency III-nitrides semiconductor solar cell. Microelectron. J. **40**, 427–434 (2009). https://doi.org/10.1016/j.mejo.2008.06.008

Bertazzi, F., Goano, M., Bellotti, E.: A numerical study of auger recombination in bulk InGaN. Appl. Phys. Lett. **97**(23), 231118 (2010)

Bhuiyan, A.G., Sugita, K., Hashimoto, A., Yamamoto, A.: InGaN solar cells: present state of the art and important challenges. IEEE J. Photovolt. **2**(3), 276–293 (2012)

Boudaoud, L., Khelifi, S., Mostefaoui, M., Rouabhia, A.K., Sahouane, N.: Numerical study of InGaN based photovoltaic by SCAPs simulation. Energy Procedia **74**, pp. 745–751, (2015). ISSN 1876-6102. https://doi.org/10.1016/j.egypro.2015.07.810

Brown, G.F., Ager, J.W., Walukiewicz, W., Wu, J., Finite element simulations of compositionally graded InGaN solar cells. Solar Energy Mater. Solar Cells **94**(3), pp. 478–483 (2010). ISSN 0927-0248

Caselli, D., Ning, C.: Full-spectrum laterally-arranged multiple-bandgap InGaN solar cells. In: 2012 38th IEEE Photovoltaic Specialists Conference, Austin, TX, pp. 002518–002520. (2012)

Dahal, R., Pantha, B., Li, J., Lin, J., Jiang, H.: InGaN/GaN multiple quantum well solar cells with long operating wavelengths. Appl. Phys. Lett. **94**(6), 063505 (2009)

Devarakonda, V., Dwivedi, A.D.D., Pandey, A., Chakrabarti, P.: Performance analysis of N^+-CdTe/n^0-$Hg_{0.824675}Cd_{0.175325}Te$/$p^+$-$Hg_{0.824675}Cd_{0.175325}Te$ n–i–p photodetector operating at 30 μm wavelength for terahertz applications. Opt. Quantum Electron. **52**, 1–19 (2020)

Durukan, I.K., Bayal, O., Kurtulus, G., Bas, Y., Gultekin, A., Ozturk, M.K., Corekei, S., Tamer, M., Ozcelik, S., Ozbay, E.: Examination of the temperature related structural defects of InGaN/GaN solar cells. Superlattices Microstruct. **86**, 379–389 (2015)

Dwivedi, A.D.D.: Analytical modeling and numerical simulation of P^+-$Hg_{0.69}Cd_{0.31}Te$/n-$Hg_{0.78}Cd_{0.22}Te$/CdZnTe heterojunction photodetector for LWIR free space optical communication system. J. Appl. Phys. **110**, 043101 (2011a)

Dwivedi, A.D.D.: Analytical modeling and ATLAS simulation of p^+-$Hg_{0.78}$ $Cd_{0.22}Te$/n-$Hg_{0.78}Cd_{0.22}Te$/CdZnTe homojunction photodetector for LWIR free space optical communication system. J. Electron Devices **9**, 396–404 (2011b)

Dwivedi, A.D.D.: Numerical simulation and spice modeling of organic thin film transistors (OTFTs). Int. J. Adv. Appl. Phys. Res. **1**, 14–21 (2014)

Dwivedi, A.D.D., Chakrabarti, P.: Modeling and analysis of photoconductive detectors based on $Hg_{1-x}Cd_xTe$ for free space optical communication. Opt. Quantum Electron. **39**, 627–641 (2007)

Dwivedi, A.D.D., Chakrabarti, P.: (2008) Modeling and ATLAS simulation of HgCdTe based MWIR photodetector for free space optical communication. In: International Conference on Recent Advances in Microwave Theory and Applications, MICROWAVE-2008, pp. 412–415

Dwivedi, A.D.D., Chakrabarti, P.: Analytical modeling and ATLAS simulation of $N+-Hg_{0.69}Cd_{0.31}Te/n_0-Hg_{0.78}Cd_{0.22}Te/p^+Hg_{0.78}Cd_{0.22}Te$ p–i–n photodetector for long wavelength free space optical communication. Optoelectron. Adv. Mater. Rapid Commun. **4**, 480–497 (2010)

Dwivedi, A.D.D., Chakrabarti, P.: Sensitivity analysis of an $Hg_{1-x}Cd_xTe$ based photoconductive receiver for long wavelength free space optical communication at 9.6 μm. J. Electron Devices **9**, 390–395 (2011)

Dwivedi, A.D.D., Chakrabarti, P.: Analytical modeling and numerical simulation of $Hg_{1-x}Cd_xTe$ based $N^+n^0p^+$Photodetector for MWIR free space optical communication. Int. J. Adv. Appl. Phys. Res. **2**, 20–27 (2015)

Dwivedi, A.D.D., Kumari, P.: TCAD simulation and performance analysis of single and dual gate OTFTs. Surf. Rev. Lett. **27**(05), 1950145 (2020). https://doi.org/10.1142/S0218625X19501452

Dwivedi, A.D.D., Mittal, A., Agrawal, A., Chakrabarti, P.: Analytical modeling and ATLAS simulation of N^+-InP/n^0-$In_{0.53}Ga_{0.47}As/p^+In_{0.53}Ga_{0.47}As$ p–i–n photodetector for optical fiber communication. Infrared Phys. Technol. **53**(4), 236–245 (2010)

Dwivedi, A.D.D., Dwivedi, R.D., Dwivedi, R.D., Vyas, S., Chakrabarti, P.: Numerical simulation of P3HT based organic thin film transistors (OTFTs). Int. J. Microelectron. Digit. Integr. Circuits **1**(2), 13–20 (2015a)

Dwivedi, A.D.D., Pranav, A., Gupta, G., Chakrabarti, P.: Numerical simulation of HgCdTe based simultaneous MWIR/LWIR photodetector for free space optical communication. Int. J. Adv. Appl. Phys. Res. **2**, 37–45 (2015b)

Dwivedi, A.D.D., Jain, S.K., Dwivedi, R.D., Dadhich, S.: Numerical simulation and compact modeling of low voltage pentacene based OTFTs. J Sci Adv Mater Devices **4**(4), 561–567 (2019)

Dwivedi, A.D.D., Jain, S.K., Dwivedi, R.D., Dadhich, S.: Numerical simulation and compact modeling of thin film transistors for flexible electronics. In: INTECK book on Hybrid Nanomaterials: Flexible Electronics Materials, June, INTECK, UK, (2020). ISBN: 978-1-83880-338-4. https://doi.org/10.5772/intechopen.90301

Farahmand, M., et al.: Monte Carlo simulation of electron transport in the III-nitride wurtzite phase materials system: binaries and ternaries. IEEE Trans. Electron Devices **48**(3), 535–542 (2001)

Gherasoiu, I., Yu, K.M., Reichertz, L.A., Walukiewicz, W.: InGaN doping for high carrier concentration in plasma-assisted molecular beam epitaxy. Physica Status Solidi (c) **11**(3–4), 381–384 (2014)

Hamzaoui, H., Bouazzi, A.S., Rezig, B.: Theoretical possibilities of $In_xGa_{1-x}N$ tandem PV structures. Sol. Energy Mater. Sol. Cells **87**(1–4), 595–603 (2005)

Islam, M.R., Hasan, M.T., Bhuiyan, A.G., Islam, M.R., Yamamoto, A.: Design and performance of $In_xGa_{1-x}N$-based MJ solar cells. IETECH J. Electr. Anal. **2**, 244–249 (2008)

Jani, O. et al.: Characterization and analysis of InGaN photovoltaic devices. In: Conference Record of the Thirty-First IEEE Photovoltaic Specialists Conference, 2005, Lake Buena Vista, FL, USA, pp. 37–42. (2005)

Kazazis, S.A., Papadomanolaki, E., Androulidaki, M.: M kayambaki, E Iliopoulos, Optical properties of InGaN thin films in the entire composition range. J. Appl. Phys. **123**(12), 125101 (2018). https://doi.org/10.1063/1.5020988

Li, J., Li, F., Lin, S., Zhong, S., Wei, Y., Meng, X., Shen, X.: Theoretical study on $In_xGa_{1-x}N$/Si heterojunction solar cells. In: Proceedings of SPIE 7409, Thin Film Solar Technology, 740910 (20 August 2009)

Lin, S., Zeng, S., Cai, X., Zhang, J., Wu, S., Sun, L., Zhang, B.: Simulation of doping levels and deep levels in InGaN-based single-junction solar cell. J. Mater. Sci. **47**(11), 4595–4603 (2012)

Matioli, E., Neufeld, C., Iza, M., Cruz, S.C., Al-Heji, A.A., Chen, X., Farrell, R.M., Keller, S., DenBaars, S., Mishra, U., et al.: High internal and external quantum efficiency InGaN/GaN solar cells. Appl. Phys. Lett. **98**(2), 021102 (2011)

Meng, Z., Bhattacharya, P., Wei, G., Banerjee, A., Mg doping of GaN grown by plasma-assisted molecular beam epitaxy under nitrogen-rich conditions. Appl. Phys. Lett. **96**(13), (2010)

Mesrane, A., Rahmoune, F., Mahrane, A., Oulebsir, A.: Design and simulation of InGaN p–n junction solar cell. Int. J. Photoenergy **2015**, Article ID 594858. http://dx.doi.org/10.1155/2015/594858

Nawaz, M., Ahmad, A.: A TCAD-based modeling of GaN/InGaN/Si solar cells. Semicond. Sci. Technol. **27**(3), Article ID 035019 (2012)

Polyakov, A.Y., Pearton, S., Frenzer, P., Ren, F., Liu, L., Kim, J.: Radiation effects in GaN materials and devices. J. Mater. Chem. C **1**(5), 877–887 (2013)

Ryu, H.-Y., Kim, H.-S., Shim, J.-I.: Rate equation analysis of efficiency droop in InGaN light-emitting diodes. Appl. Phys. Lett. **95**(8), 081114 (2009)

Selberherr, S.: Analysis and Simulation of Semiconductor Devices. Springer, Berlin (2012)
Schwierz, F.: An electron mobility model for wurtzite GaN. Solid State Electron. **49**(6), 889–895 (2005)
Silvaco Data systems, Atlas User's manual version, Silvaco Data Systems (2018)
Sinha, N., Chandra, V., Dwivedi, A.D.D.: TCAD based assessment and performance optimization of ZnO/Si heterojunction based thin-film solar cell. Int. J. Adv. Appl. Phys. Res. **3**(2), 26–33 (2016a)
Sinha, N., Chandra, V., Dwivedi, A.D.D.: Modeling and simulation of n-ZnO/i-ZnO/Si p–i–n heterojunction solar cell. Int. J. Microelectron. Digit. Integr. Circuits **2**(2), 1–5 (2016b)
Vilbois, L.A., Cheknane, A., Bensaoula, A., Boney, C., Benouaz, T.: Simulation of a solar cell based on InGaN. Energy Procedia **18**, pp. 795–806, (2012). ISSN 1876-6102. https://doi.org/10.1016/j.egypro.2012.05.095
Wu, J., Walukiewicz, W., Yu, K.M., Shan, W., Ager III, J.W., Haller, E.E., Lu, H., Schaff, W.J., Metzger, W.K., Kurtz, S.: Superior radiation resistance of $In_{1-x}Ga_xN$ alloys: full-solar-spectrum photovoltaic material system. J. Appl. Phys. **94**(10), 6477–6482 (2003)
Yamamoto, A., Sugita, K., Bhuiyan, A., Hashimoto, A., Narita, N.: Metalorganic vapor-phase epitaxial growth of InGaN and InAlN for multijunction tandem solar cells. Mater. Renew. Sustain. Energy **2**(2), 1–9 (2013)
Zhang, X., Wang, X., Xiao, H., Yang, C., Ran, J., Wang, C., Hou, Q., Li, J.: Simulation of $In_{0.65}Ga_{0.35}N$ single-junction solar cell. J. Phys. D Appl. Phys. **40**(23), 7335–7338 (2007)

Publisher's Note Springer Nature remains neutral with regard to jurisdictional claims in published maps and institutional affiliations.